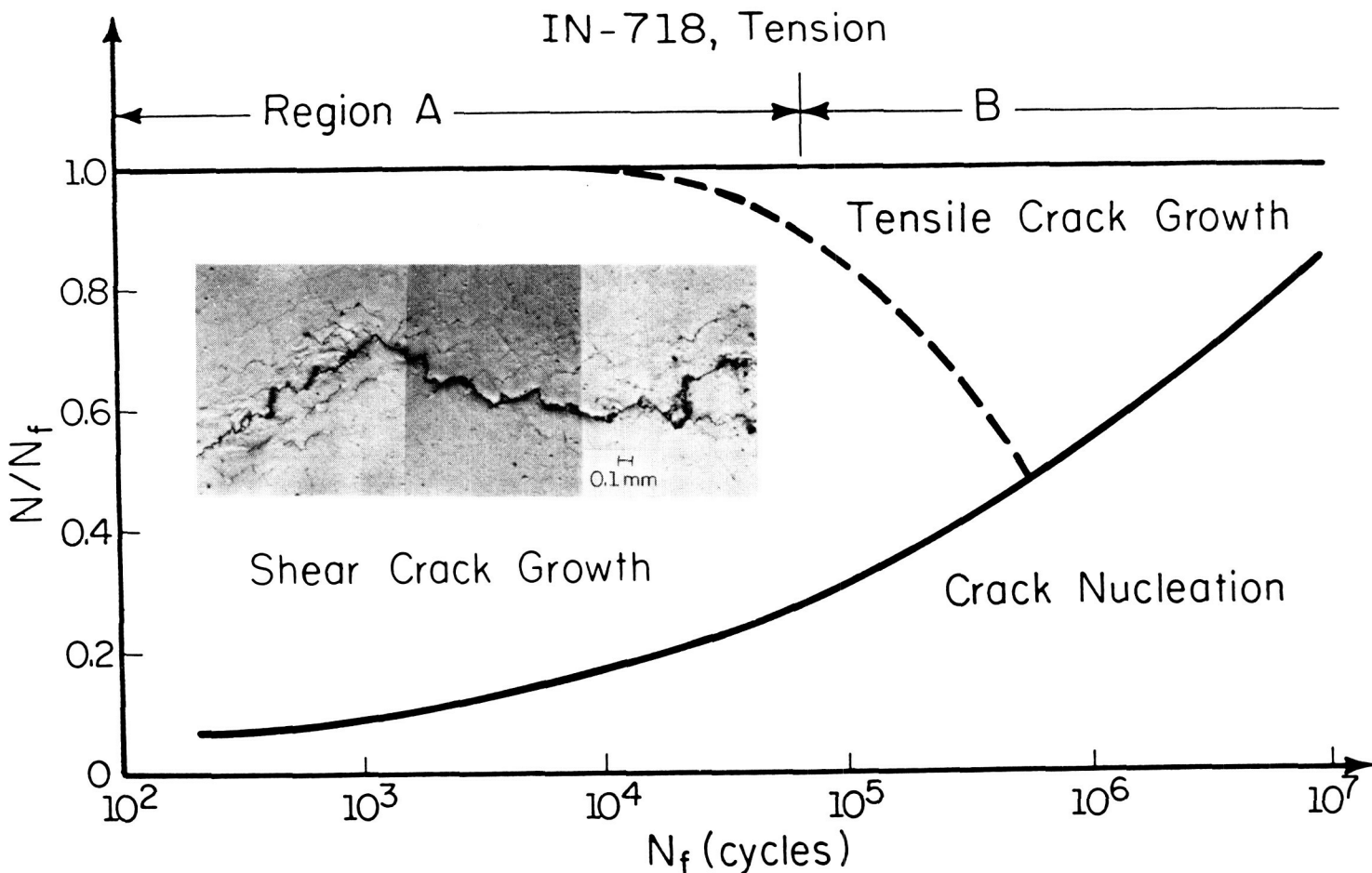# FATIGUE DAMAGE MAPPING

Darrell Socie
Department of Mechanical and Industrial Engineering
University of Illinois at Urbana-Champaign

Observations of fatigue crack nucleation and early growth are presented. The state of stress/strain has been shown to play a significant role in this process. Early growth occurs on planes experiencing the largest range of shear strain (Mode II) or normal strain (Mode I) depending on the stress state, strain amplitude, and microstructure. These observations have been summarized in a fatigue damage map for each material. These maps provide regions where one fatigue failure mode dominates the behavior. Each failure mechanism results in a different failure mode. Once the expected failure mode has been identified, bulk deformation models based on the cyclic stresses and strains can be used to obtain reliable estimates of fatigue lives for complex loading situations.

EXECUTIVE OVERVIEW OF FATIGUE DAMAGE MAPPING

A fatigue damage map for Inconel 718 loaded in cyclic tension is given below. The vertical scale is presented in terms of life fraction and the horizontal scale in terms of fatigue life. The solid line represents the first observation of a surface crack 100 μm long and serves as a demarcation between initiation and growth. The dashed line represents the demarcation between crack growth on planes of maximum shear strain amplitude and crack growth on planes of maximum principal strain amplitude. Region A is characterized by shear initiation followed by extensive shear crack growth with final failure occurring by a linking of shear cracks similar to the tearing of perforated paper. Region B is characterized by shear initiation followed by crack growth along the principal stress direction. A third region is often observed at long lives and small strains where there is no observable initiation or shear initiation resulting in nonpropagating cracks. A separate damage model is required for each region.

EXECUTIVE OVERVIEW OF FATIGUE DAMAGE MAPPING

The damage maps indicate that a shear strain based theory is most appropriate for this material for lives below about 10^5 cycles. One such damage parameter has been proposed by Fatemi and Socie (1985)

$$\gamma \left(1 + \frac{\sigma_n}{\sigma_y}\right)$$

Two parameters are considered to cause fatigue damage. The primary damage is caused by the cyclic shear strains (γ). Stresses normal to the cyclic shear strain tend to open any microcracks and enhance their growth. Hence the second term can be interpreted as including crack closure effects. The term also includes effects from any additional cyclic hardening that is often observed during nonproportional loading. The stress normal to the shear crack (σ_n) is normalized with the yield strength (σ_y) to retain the dimensionless features of strain. In this formulation no fatigue damage is computed for planes in the material that do not experience cyclic shear strain. Results are presented for a wide variety of loading histories including tension, torsion, biaxial tension, and tests with complex multiaxial mean stresses. Both proportional and nonproportional tests are included. This degree of correlation is only possible because the damage mechanism does not change for the variety of tests considered here.
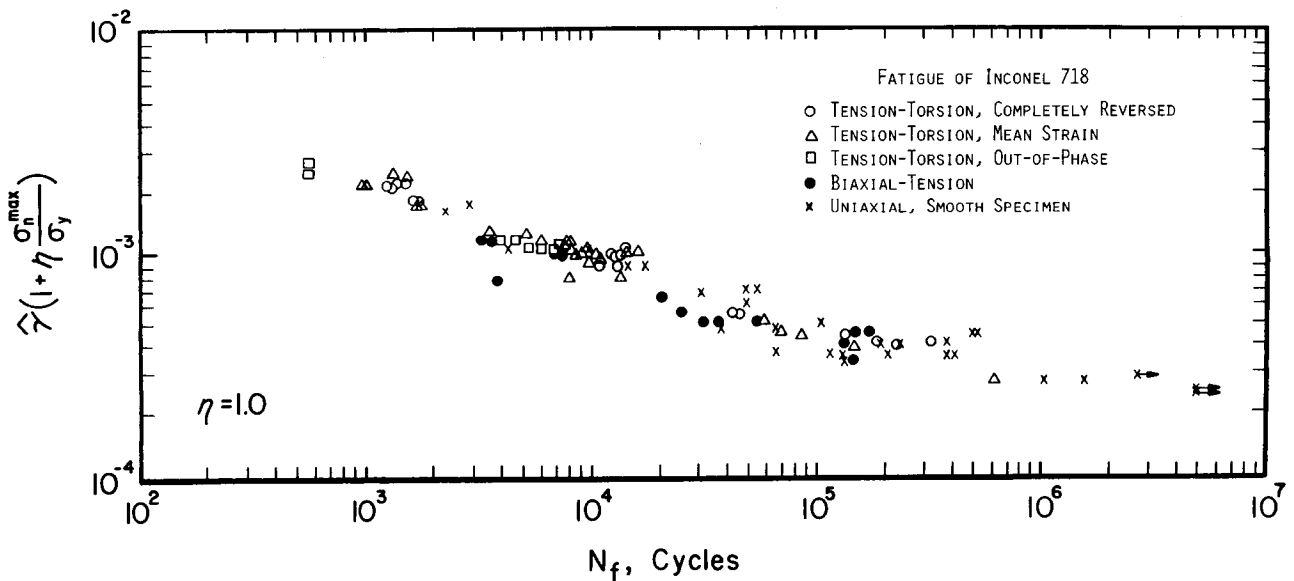
FATIGUE DAMAGE MAP FOR INCONEL 718

Test data from individual stress states are summarized in the fatigue damage map for Inconel 718 given below. The vertical axis has now been plotted in terms of hydrostatic stress normalized by the maximum principal stress. Torsion, tension and biaxial tension have values of 0, 1/3, and 2/3, respectively. Regions of similar fatigue failure modes are given. Little data exists for the case of biaxial tension and these lines are shown as dashed. The map shows that over a wide range of stress states and strain amplitudes the primary failure mechanism is one of shear crack growth. The x symbols in the preceding figure that fall to the right of the central tendency of the test data represent large compressive mean stress tests. This type of behavior is expected since the fatigue damage map shows a transition from shear to tensile dominated behavior at longer lives. In this failure mode, compressive stresses would retard crack growth and prolong fatigue lives.
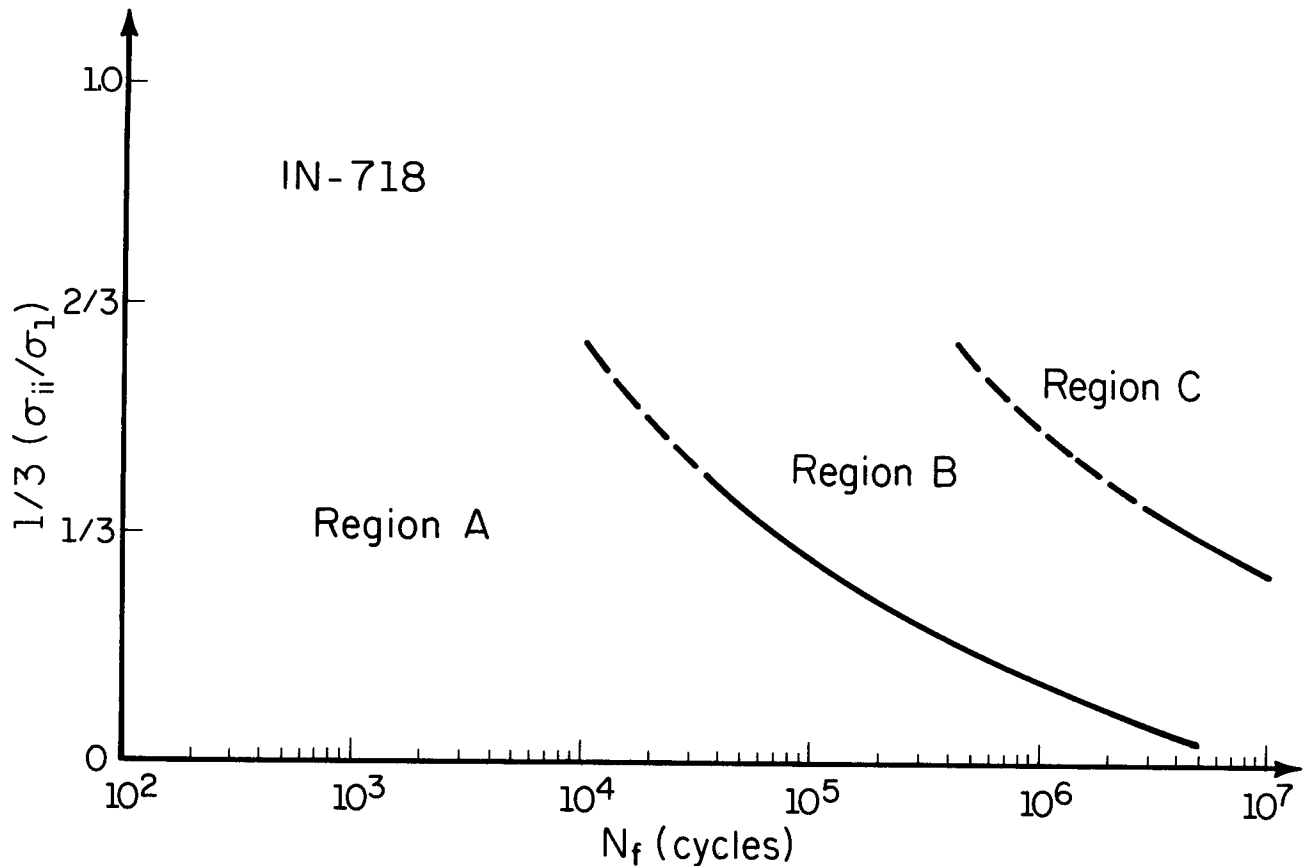
FATIGUE DAMAGE MAP FOR 304 STAINLESS STEEL

The fatigue damage map for 304 stainless steel is given below. Note that the region of shear behavior found in Inconel 718 is restricted to a narrow range in 304 stainless steel. There is a large region of tensile dominated behavior. It is suggested that a tensile strain based model is most appropriate here. One such model has been proposed by Smith, et al. (1970), and has found widespread use in uniaxial fatigue situations.

$$\sigma_{max} \, \varepsilon_a$$

Two parameters are considered to be the driving force for fatigue damage. The maximum principal strain amplitude, ε_a, and the tensile stress normal to that plane, σ_{max}.

3-217
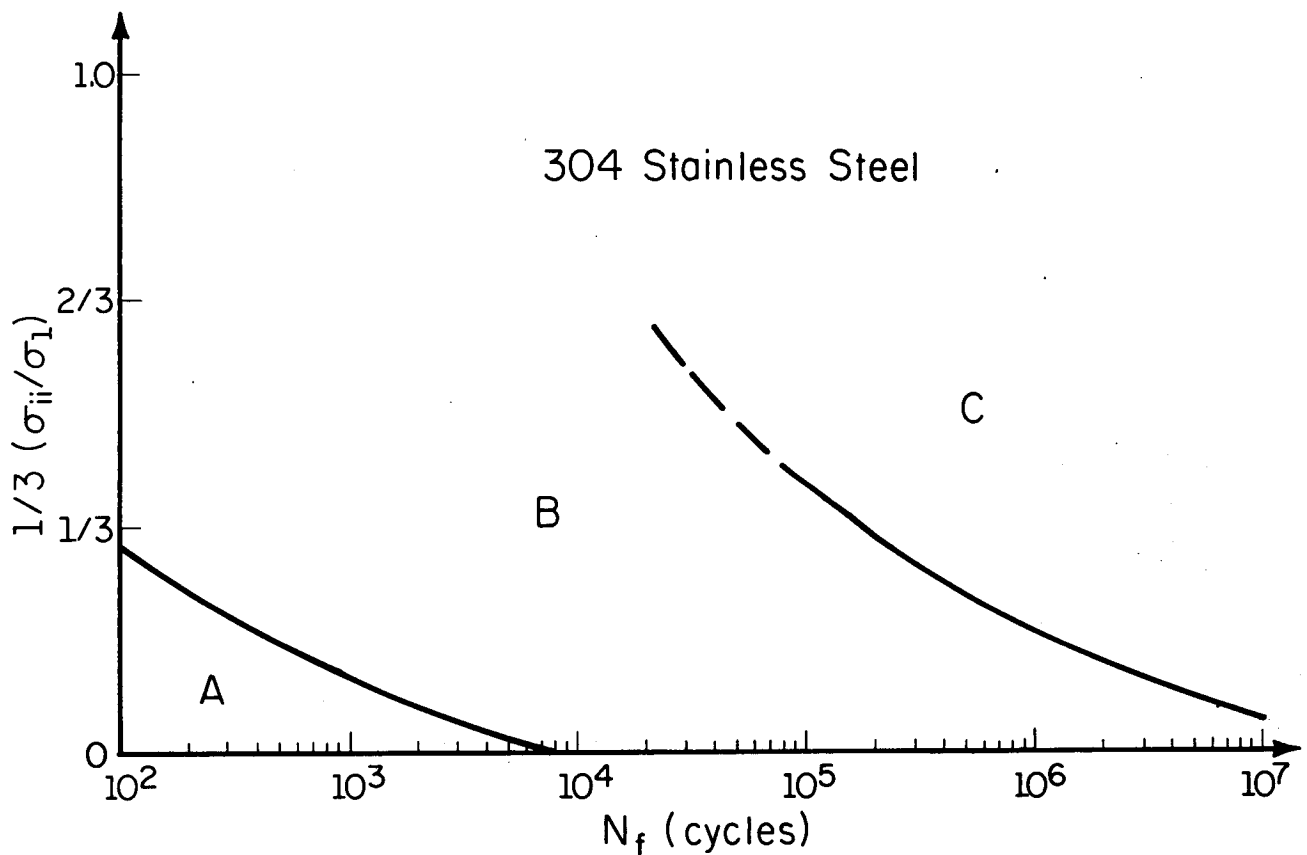
LIFE ESTIMATIONS FOR 304 STAINLESS STEEL

Test data for 304 stainless steel from Socie (1987) for both proportional and nonproportional tests are given below. This material cyclically hardens under nonproportional loading to a stable stress level that is nearly double that of a proportional test. The increase in cyclic stress is very damaging and must be accounted for in the model. For the same total strain range, uniaxial loading has the largest plastic strain range and longest life. Nonproportional loading tests have the smallest plastic strain range, largest stress range and shortest life.
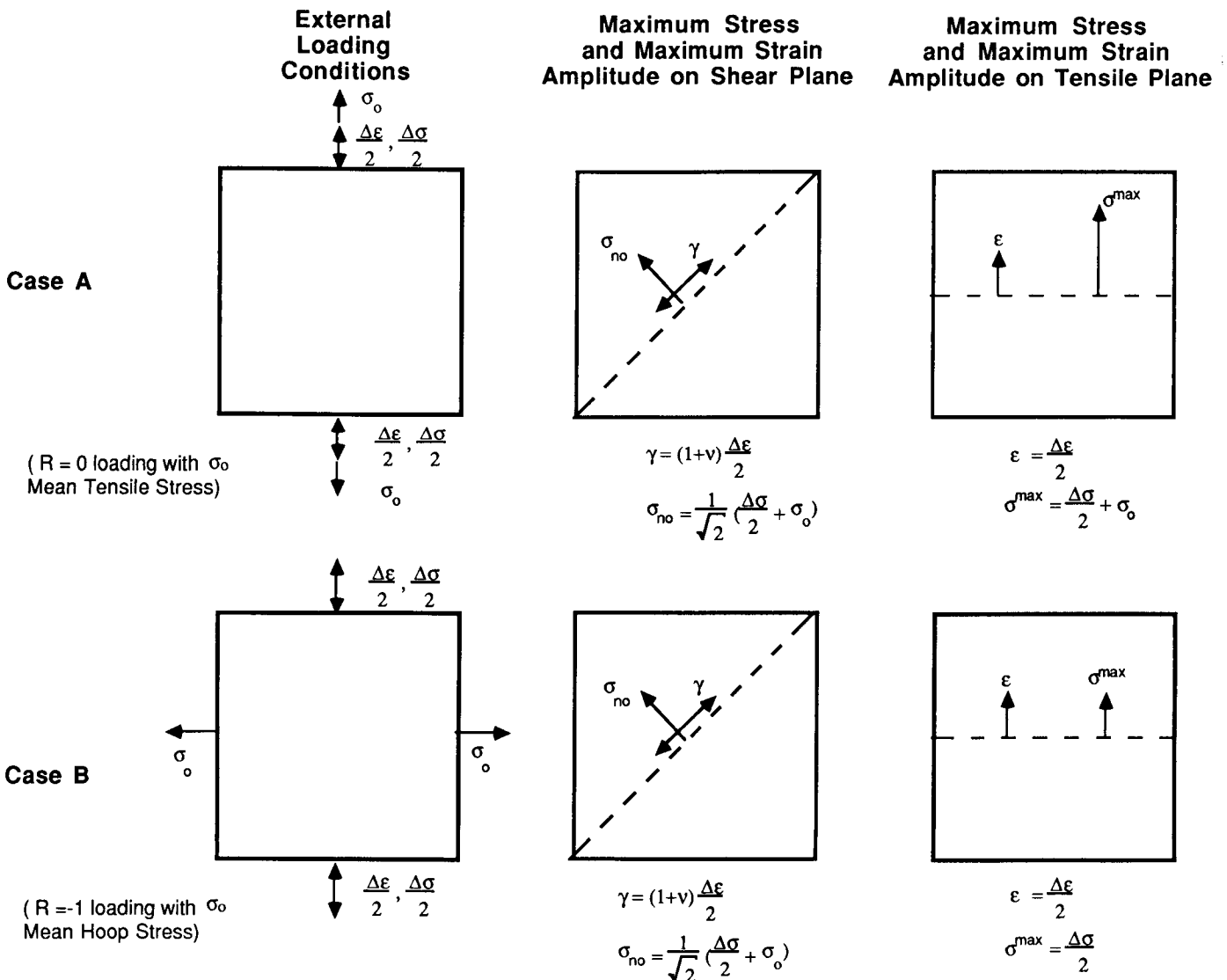

304 Stainless Steel

(y-axis: $\sigma_1^{max} \Delta\epsilon_1/2$)

(x-axis: $N_{1.0}$)
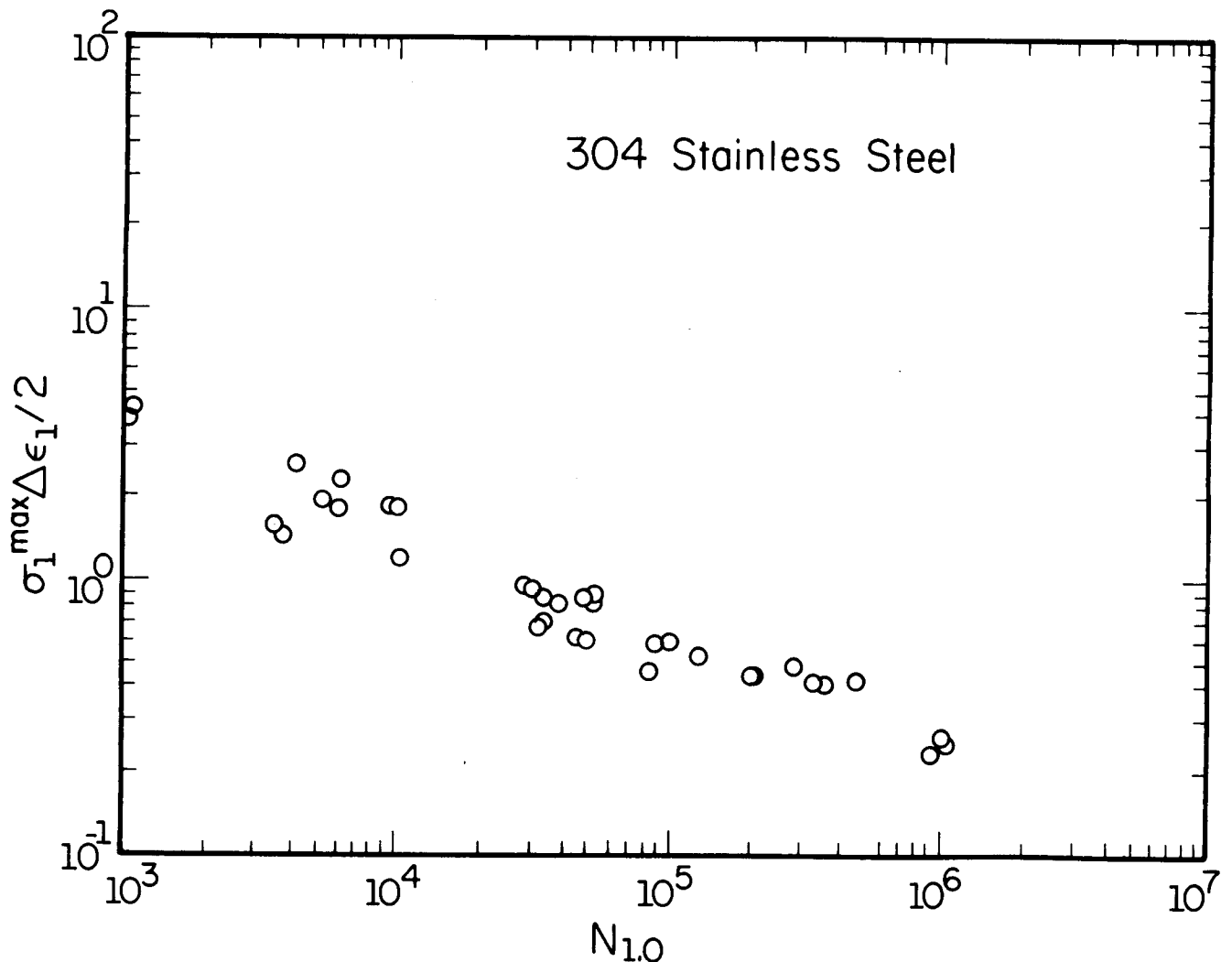
Two loading cases that have the same shear damage parameter are given below. Consider a standard uniaxial test specimen, Case A, tested in zero to maximum strain cycling. A tensile mean stress σ_o will result. Now consider a second test, Case B, of a tubular specimen tested with the same axial strain range only in completely reversed loading. The magnitude of the mean stress in the first test is applied as a hoop stress in the second test. Since the shear damage parameter is the same for both tests the fatigue lives would be expected to be similar for a material that fails in a shear mode. Note that the tensile damage parameter for the second test is much lower since there is no mean stress in the plane experiencing the largest range of cyclic principal strain. Results for Inconel 718 are as follows:

$\Delta\varepsilon/2$	σ_o	Case A	Case B
0.0005	270	4245	6735
		9768	7221

These tests confirm the selection of the damage parameter since the lives are the same for both tests. The tensile model predicts an increase in fatigue life for Case B that was not observed experimentally.

	External Loading Conditions	Maximum Stress and Maximum Strain Amplitude on Shear Plane	Maximum Stress and Maximum Strain Amplitude on Tensile Plane

Case A

(R = 0 loading with σ_o Mean Tensile Stress)

$$\gamma = (1+v)\frac{\Delta\varepsilon}{2}$$

$$\sigma_{no} = \frac{1}{\sqrt{2}}(\frac{\Delta\sigma}{2}+\sigma_o)$$

$$\varepsilon = \frac{\Delta\varepsilon}{2}$$

$$\sigma^{max} = \frac{\Delta\sigma}{2}+\sigma_o$$

Case B

(R = -1 loading with σ_o Mean Hoop Stress)

$$\gamma = (1+v)\frac{\Delta\varepsilon}{2}$$

$$\sigma_{no} = \frac{1}{\sqrt{2}}(\frac{\Delta\sigma}{2}+\sigma_o)$$

$$\varepsilon = \frac{\Delta\varepsilon}{2}$$

$$\sigma^{max} = \frac{\Delta\sigma}{2}$$

REFERENCES

Fatemi, A., and Socie, D. F. (1987), "A Critical Plane Approach to Multiaxial Fatigue Damage Including Out-of-Phase Loading," accepted for publication in Fatigue and Fracture Engineering Materials and Structures.

Smith, R. N., Watson, P., and topper, T. H. (1970), "A Stress-Strain Function for the Fatigue of Metals," Journal of Materials, JMLSA, Vol. 5, No. 4, pp. 767-778.

Socie, D. F. (1987), "Multiaxial Fatigue Damage Models," Journal of Engineering Materials and Technology, Vol. 109, No. 4, pp. 293-298.